

# Graph Neural Networks with Convolutional ARMA Filters

Filippo Maria Bianchi<sup>1</sup> Daniele Grattarola<sup>2</sup> Cesare Alippi<sup>2,3</sup> Lorenzo Livi<sup>4,5</sup>

## Abstract

Popular graph neural networks implement convolution operations on graphs based on polynomial filters defined in the spectral domain. In this paper, we propose a novel graph convolutional layer inspired by the auto-regressive moving average (ARMA) filters that, compared to the polynomial ones, are more robust and provide a more flexible graph frequency response. We propose a neural network implementation of the ARMA filter with a recursive and distributed formulation, obtaining a convolutional layer that is efficient to train, localized in the node space, and can be transferred to new graphs unseen during training. We report a spectral analysis of the proposed trainable filter, as well as experiments on four major downstream tasks: semi-supervised node classification, graph signal classification, graph classification, and graph regression. The results show that ARMA filters bring significant improvements over graph neural networks based on polynomial filters.

## 1. Introduction

Graph Neural Networks (GNNs) are a class of models lying at the intersection between deep learning and methods for structured data, which perform inference on discrete objects (nodes) by accounting for arbitrary relationships (edges) among them (Battaglia et al., 2018). A GNN combines node features within local neighborhoods on the graph to learn graph embeddings (Perozzi et al., 2014; Duvenaud et al., 2015; Yang et al., 2016; Hamilton et al., 2017; Bacciu et al., 2018), or to directly perform inference tasks by mapping the node features into categorical labels or real

values (Scarselli et al., 2009; Klicpera et al., 2019).

Of particular interest for this work are those GNNs that implement a convolution operation in the spectral domain with a nonlinear trainable filter (Bruna et al., 2013; Henaff et al., 2015), which selectively amplifies the graph Fourier coefficients of the node features and map the node features in a new space. To avoid the expensive spectral decomposition and projection in the frequency domain, state-of-the-art GNNs approximate graph filters with finite order polynomials (Defferrard et al., 2016; Kipf & Welling, 2016a;b). Polynomial filters have a finite impulse response and realize a weighted moving average filtering of graph signals on local node neighbourhoods (Tremblay et al., 2018), thus allowing for fast distributed implementations based on Chebyshev polynomials and Lanczos iterations (Sussjara et al., 2015; Defferrard et al., 2016; Liao et al., 2019). Despite their attractive computational efficiency, polynomial filters are sensitive to changes in the graph signal (an instance of the node features) or in the underlying graph structure (Isufi et al., 2016). Moreover, due to their smoothness, polynomial filters cannot model sharp changes in the frequency response (Tremblay et al., 2018). A more versatile class of filters is the family of Auto-Regressive Moving Average filters (ARMA) that provide a larger variety of frequency responses (Narang et al., 2013).

In this paper, we address the limitations of existing graph convolutional layers in modeling a desired filter response, and propose a novel GNN convolutional layer based on the ARMA filter. Our ARMA layer implements a non-linear and trainable graph filter that generalizes the graph convolutional layers based on polynomial filters, and provides the GNN with enhanced modeling capability thanks to a flexible design of the filter’s frequency response. Contrarily to polynomial filters, traditional ARMA filters are not localized in node space, making their implementation inefficient. To address this scalability issue, the proposed ARMA layer relies on a recursive formulation, which leads to a fast and distributed implementation that exploits efficient sparse operations on tensors. The resulting filters are not learned in the Fourier space induced by a given Laplacian, but are localized in the node space and independent from the underlying graph structure. This allows our GNN to handle graphs with unseen topologies in inductive inference tasks.

<sup>1</sup>NORCE, The Norwegian Research Institute, Norway

<sup>2</sup>Faculty of Informatics, Università della Svizzera Italiana, Switzerland <sup>3</sup>Dept. of Electronics, Information, and Bioengineering, Politecnico di Milano, Italy <sup>4</sup>Dept. of Computer Science and Mathematics, University of Manitoba, Canada

<sup>5</sup>Dept. of Computer Science, University of Exeter, United Kingdom. Correspondence to: Filippo Maria Bianchi <filippom-bianchi@gmail.com>.

To assess the performance of the proposed ARMA layer, we apply it to semi-supervised node classification, graph signal classification, graph classification, and graph regression tasks. Results show that the proposed GNN with ARMA layers outperforms GNNs based on polynomial filters in several downstream tasks.

## 2. Spectral filtering on graphs

We assume a graph with  $M$  nodes to be characterized by a symmetric adjacency matrix  $\mathbf{A} \in \mathbb{R}^{M \times M}$  and refer to *graph signal*  $\mathbf{X} \in \mathbb{R}^{M \times F}$  as the instance of all features (vectors in  $\mathbb{R}^F$ ) associated with the graph nodes. Let  $\mathbf{L} = \mathbf{I}_M - \mathbf{D}^{-1/2} \mathbf{A} \mathbf{D}^{-1/2}$  be the symmetrically normalized Laplacian ( $\mathbf{D}$  is the degree matrix), with spectral decomposition  $\mathbf{L} = \sum_{m=1}^M \lambda_m \mathbf{u}_m \mathbf{u}_m^T$ . A graph filter is a linear operator that modifies the components of  $\mathbf{X}$  on the eigenvectors basis of  $\mathbf{L}$ , according to a frequency response  $h$  acting on each eigenvalue  $\lambda_m$ . The filtered graph signal reads

$$\begin{aligned} \bar{\mathbf{X}} &= \sum_{m=1}^M h(\lambda_m) \mathbf{u}_m \mathbf{u}_m^T \mathbf{x}_m \\ &= \mathbf{U} \text{diag}[h(\lambda_1), \dots, h(\lambda_M)] \mathbf{U}^T \mathbf{X} \end{aligned} \quad (1)$$

This formulation inspired the seminal work of (Bruna et al., 2013) that implemented spectral graph convolutions in a neural network. Their GNN learns end-to-end the parameters of each filter implemented as  $h = \mathbf{B}\mathbf{c}$ , where  $\mathbf{B} \in \mathbb{R}^{M \times K}$  is a cubic B-spline basis and  $\mathbf{c} \in \mathbb{R}^K$  is a vector of control parameters. Such filters are not localized, since the full projection on the eigenvectors yields paths of infinite length and the filter accounts for interactions of each node with the whole graph, rather than those limited to the node neighborhood. Since this contrasts with the local design of classic convolutional filters, (Henaff et al., 2015) introduced a parametrization of the spectral filters with smooth coefficients to achieve spatial localization. However, the main issue with such spectral filtering (Eq.1) is the computational complexity: not only the eigendecomposition of  $\mathbf{L}$  is computationally expensive, but a double product with  $\mathbf{U}$  must be computed whenever the filter is applied. Notably,  $\mathbf{U}$  in (1) is full even when  $\mathbf{L}$  is sparse. Finally, since spectral filters depend on their specific Laplacian spectrum, they cannot be applied to graphs with a different structure.

### 2.1. GNNs based on polynomial filters and limitations

The desired filter response  $h(\lambda)$  can be approximated by a polynomial of order  $K$ ,

$$h_{\text{POLY}}(\lambda) = \sum_{k=0}^K w_k \lambda^k, \quad (2)$$

which performs a weighted moving average of the graph signal (Tremblay et al., 2018). Polynomial filters are localized in space, since the output at each node in the filtered signal is a linear combination of the nodes in its  $K$ -hop neighbourhood. These filters overcome important limitations of the spectral formulation, by avoiding the eigen-decomposition and by not relying on a fixed Laplacian spectrum, making them suitable for inductive inference tasks on graphs with different structures (Zhang et al., 2018).

Compared to conventional polynomials, Chebyshev polynomials attenuate unwanted oscillations around the cut-off frequencies (Shuman et al., 2011). Fast localized GNN filters can approximate the desired filter response by means of the Chebyshev expansion  $T_k(x) = 2xT_{k-1}(x) - T_{k-2}(x)$  (Defferrard et al., 2016), resulting in convolutional layers that perform the filtering operation

$$\bar{\mathbf{X}} = \sigma \left( \sum_{k=0}^{K-1} T_k(\tilde{\mathbf{L}}) \mathbf{X} \mathbf{W}_k \right), \quad (3)$$

where  $\tilde{\mathbf{L}} = 2\mathbf{L}/\lambda_{\max} - \mathbf{I}_M$ ,  $\sigma$  is a non-linear activation (e.g., ReLU), and  $\mathbf{W}_k \in \mathbb{R}^{F_{\text{in}} \times F_{\text{out}}}$  are the  $k$  trainable weight matrices that map the node's features from an input space  $\mathbb{R}^{F_{\text{in}}}$  to a new space  $\mathbb{R}^{F_{\text{out}}}$ .

A first-order polynomial filter has been adopted by (Kipf & Welling, 2016a) for semi-supervised node classification. They propose a GNN called Graph Convolutional Network (GCN), where the convolutional layer is a simplified version of a Chebyshev filter, obtained from (3) by considering only  $K = 1$  and setting  $\mathbf{W} = \mathbf{W}_0 = -\mathbf{W}_1$

$$\bar{\mathbf{X}} = \sigma \left( \hat{\mathbf{A}} \mathbf{X} \mathbf{W} \right). \quad (4)$$

Additionally,  $\tilde{\mathbf{L}}$  is replaced by  $\hat{\mathbf{A}} = \tilde{\mathbf{D}}^{-1/2} \tilde{\mathbf{A}} \tilde{\mathbf{D}}^{-1/2}$ , with  $\tilde{\mathbf{A}} = \mathbf{A} + \gamma \mathbf{I}_M$  (usually,  $\gamma = 1$ ). In respect to  $\tilde{\mathbf{L}}$ ,  $\hat{\mathbf{A}}$  contains self-loops that compensate for the removal of the term of order 0 in the polynomial filter, by ensuring that a node is part of its first order neighbourhood and that its features are preserved after the convolution. Higher-order node neighbourhoods can be reached by stacking multiple GCN layers. However, since each GCN layer performs a Laplacian smoothing, after few convolutions the node features becomes too smoothed over the graph (Li et al., 2018).

The output of an  $k$ -degree polynomial filter is a linear combination of the input within each vertex's  $k$ -hop neighbourhood. Since the input beyond the  $k$ -hop neighborhood has no impact on the output, to represent global structures on the graph it is necessary to use high-degree polynomials. However, high-degree polynomials have poor interpolatory and extrapolatory performance around the known graph frequencies, are sensitive to small changes/noise on

the graph topology (which leads to overfitting), and require more computational power to be computed/learned (Isufi et al., 2016). Moreover, since polynomial are smooth, it not possible to model filter responses with sharp changes.

## 2.2. Rational filters in graph signal processing

An ARMA filter can approximate well any desired filter response  $h(\lambda)$  thanks to a rational design that allows to model a larger variety of filter shapes, compared to a polynomial filter (Tremblay et al., 2018). The filter response of an ARMA filter of order  $K$ , denoted in the following as  $\text{ARMA}_K$ , reads

$$h_{\text{ARMA}_K}(\lambda) = \frac{\sum_{k=0}^K p_k \lambda^k}{1 + \sum_{k=1}^K q_k \lambda^k}, \quad (5)$$

which, in the node domain, translates to the following filtering relation in the node space

$$\bar{\mathbf{X}} = \frac{\left(\sum_{k=0}^K p_k \mathbf{L}^k\right) \mathbf{X}}{1 - \sum_{k=1}^K q_k \mathbf{L}^k}. \quad (6)$$

To illustrate how an ARMA filter accounts for larger sections of the graph compared to a polynomial filter of the same order, consider a dynamic process on the graph  $\mathbf{x}^{(0)}, \mathbf{x}^{(1)}, \mathbf{x}^{(2)}, \dots$  defined by the map  $\mathbf{x}^{(t+1)} = \mathbf{L}\mathbf{x}^{(t)}$ . The representation  $\bar{\mathbf{x}}^{(t)}$  given by a polynomial filter is

$$\bar{\mathbf{x}}^{(t)} = \mathbf{x}^{(t)} + p_1 \mathbf{x}^{(t+1)} + p_2 \mathbf{x}^{(t+2)} + \dots$$

which is a regression on the evolution of the diffusion process on the graph, starting from the current state. The ARMA filter introduces an additional term

$$\mathbf{x}^{(t)} = q_1 \bar{\mathbf{x}}^{(t+1)} + q_2 \bar{\mathbf{x}}^{(t+2)} + \dots$$

which is a regression over the (unknown) graph process driven by the representation  $\bar{\mathbf{x}}$ . This additional term makes the model more robust to noise and captures longer dynamics on the graph since  $\bar{\mathbf{x}}$  depends, in turn, on several propagation steps. By rearranging terms and using the previous map definition, we recover Eq. 6:

$$\begin{aligned} \bar{\mathbf{x}}^{(t)} &= q_1 \bar{\mathbf{x}}^{(t+1)} + q_2 \bar{\mathbf{x}}^{(t+2)} + p_1 \mathbf{x}^{(t+1)} + p_2 \mathbf{x}^{(t+2)} + \dots \\ \bar{\mathbf{x}}^{(t)} - q_1 \bar{\mathbf{x}}^{(t+1)} - q_2 \bar{\mathbf{x}}^{(t+2)} \dots &= p_1 \mathbf{x}^{(t+1)} + p_2 \mathbf{x}^{(t+2)} \dots \\ \left(1 - \sum_k q_k \mathbf{L}^k\right) \bar{\mathbf{x}}^{(t)} &= \left(\sum_k p_k \mathbf{L}^k\right) \mathbf{x}^{(t)} \end{aligned}$$

The Laplacian appearing in the denominator of (6) implies a matrix inversion and a multiplication with a dense matrix, which is inefficient to implement in a GNN. To circumvent this issue, CayleyNets (Levie et al., 2019b) approximate the

inverse with a fixed number of Jacobi iterations, by using an elaborated and computationally intensive formulation to avoid numerical instability.

To implement our GNN, we take inspiration from a more straightforward approach that completely avoids computing the inverse and approximates the effect of an  $\text{ARMA}_1$  filter by iterating until convergence the first-order recursion

$$\bar{\mathbf{X}}^{(t+1)} = a\mathbf{M}\bar{\mathbf{X}}^{(t)} + b\mathbf{X}, \quad (7)$$

where  $\mathbf{M} = \frac{1}{2}(\lambda_{\max} - \lambda_{\min})\mathbf{I} - \mathbf{L}$ . The recursive application of Eq. (7) is adopted in graph signal processing to apply a low-pass filter on a graph signal (Loukas et al., 2015; Isufi et al., 2016), but (7) is also equivalent to the recurrent update used in Label Propagation (Zhou et al., 2004) and Personalized Page Rank (Page et al., 1999) to propagate information on a graph with a restart probability.

We first analyze the frequency response of an  $\text{ARMA}_1$  filter, from the convergence of (7):

$$\bar{\mathbf{X}} = \lim_{t \rightarrow \infty} (a\mathbf{M})^t \mathbf{X}^{(0)} + b \sum_{i=0}^t (a\mathbf{M})^i \mathbf{X}. \quad (8)$$

The eigenvalues of  $\mathbf{M}$  are related to those of the Laplacian  $\mathbf{L}$  as follows:  $\mu_m = (\lambda_{\max} - \lambda_{\min})/2 - \lambda_m$ , where  $\mu_m$  and  $\lambda_m$  represent the  $m$ -th eigenvalue of  $\mathbf{M}$  and  $\mathbf{L}$ , respectively. Since  $\mu_m \in [-1, 1]$ , for  $|a| < 1$  the first term of (8),  $(a\mathbf{M})^t$ , goes to zero when  $t \rightarrow \infty$ . The second term,  $b \sum_{i=0}^t (a\mathbf{M})^i$ , represents a geometric series that converges to the matrix  $b(\mathbf{I} - a\mathbf{M})^{-1}$ , with eigenvalues  $b/(1 - a\mu_m)$ . It follows that the frequency response of the  $\text{ARMA}_1$  filter is

$$h_{\text{ARMA}_1}(\mu_m) = \frac{b}{1 - a\mu_m} = \frac{r}{\mu_m - p}, \quad (9)$$

with  $r = -\frac{b}{a}$  and  $p = \frac{1}{a}$ .

By summing  $K$   $\text{ARMA}_1$  filters it is possible to recover the effect of the  $\text{ARMA}_K$  filter in (5). The resulting filtering operation is

$$\bar{\mathbf{X}} = \sum_{k=1}^K \sum_{m=1}^M \frac{r_k}{\mu_m - p_k} \mathbf{u}_m \mathbf{u}_m^T \mathbf{x}_m, \quad (10)$$

with  $h_{\text{ARMA}_K}(\mu_m) = \sum_{k=1}^K \frac{r_k}{\mu_m - p_k}$ . Different orders ( $\leq K$ ) of the numerator and denominator in (5), are trivially obtained by setting some coefficients to 0. It follows that ARMA filters can generalize every polynomial filter, by zeroing the denominator coefficients.

## 3. The ARMA neural network layer

In graph signal processing, the filter coefficients are optimized with polynomial regression and least-square regression to reproduce a desired filter response  $h^*(\lambda)$ , which

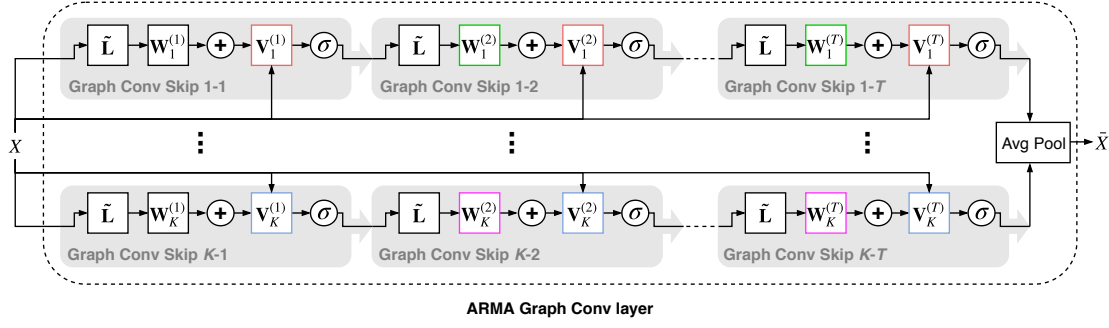


Figure 1. The ARMA convolutional layer. Same colour indicates shared weights.

must be provided *a priori* by the designer. Also, Eq. (7) must be applied many times before converging to a steady state and precautions must be taken to avoid instability during the optimization (Isufi et al., 2016).

We address these issues by proposing a formulation of the ARMA filters based on neural networks. Specifically, we implement one recursive update in (7) with a *Graph Convolutional Skip* (GCS) layer, defined as

$$\bar{\mathbf{X}}^{(t+1)} = \sigma \left( \tilde{\mathbf{L}} \bar{\mathbf{X}}^{(t)} \mathbf{W}^{(t)} + \mathbf{X} \mathbf{V}^{(t)} \right), \quad (11)$$

where  $\mathbf{W}^{(t)} \in \mathbb{R}^{F_{\text{out}}^t \times F_{\text{out}}^{t+1}}$  and  $\mathbf{V}^{(t)} \in \mathbb{R}^{F_{\text{in}} \times F_{\text{out}}^{t+1}}$  are trainable parameters, and  $\mathbf{X}$  are the initial node features. The modified Laplacian matrix  $\tilde{\mathbf{L}} = \mathbf{I} - \mathbf{L}$  is derived by setting  $\lambda_{\min} = 0$  and  $\lambda_{\max} = 2$  in  $\mathbf{M}$ . This is a reasonable simplification, since the spectrum of  $\mathbf{L}$  lies in  $[0, 2]$  and the trainable parameters  $\mathbf{W}^{(t)}$  and  $\mathbf{V}^{(t)}$  can compensate for the small offset introduced.

Thanks to the non-linearities and a larger set of trainable parameters, it is possible to approximate the response of any  $\text{ARMA}_1$  filter by stacking only a small (fixed) number  $T$  of GCS layers. In this way, it is possible to avoid the convergence issues of the original formulation and obtain a very fast and stable implementation of the filter. Additionally, we do not require to specify the target response  $h^*(\lambda)$ , since the filter parameters are learned end-to-end from the data, by optimizing a loss function with gradient descent.

Each GCS layer is localized in the node space, as it performs a filtering operation only through local exchanges between neighboring nodes on the graph and, through the skip connection, also with the initial node features. The computational complexity (in time and space) of the GCS layer is linear in the number of edges, and can be efficiently implemented as a sparse product of  $\mathbf{L}$  and  $\mathbf{X}$ .

The output of the  $\text{ARMA}_K$  convolutional layer is obtained by combining  $K$  parallel stacks of  $T$  GCS layers

$$\bar{\mathbf{X}} = \frac{1}{K} \sum_{k=1}^K \bar{\mathbf{X}}_k^{(T)}, \quad (12)$$

where  $\bar{\mathbf{X}}_k^{(T)}$  is the last output of the  $k$ -th stack (see Fig. 1).

All the GCS layers in each stack share the same parameters, except for  $\mathbf{W}_k^{(1)} \in \mathbb{R}^{F_{\text{in}} \times F_{\text{out}}}$  in the first layer, which performs a different mapping from the input to the output node features domain. Namely,  $\mathbf{W}_k^{(t)} = \mathbf{W}_k^{(t+1)} = \mathbf{W}_k \in \mathbb{R}^{F_{\text{out}} \times F_{\text{out}}}$ ,  $\forall t > 1$  and  $\mathbf{V}_k^{(t)} = \mathbf{V}_k^{(t+1)} = \mathbf{V}_k \in \mathbb{R}^{F_{\text{in}} \times F_{\text{out}}}$ ,  $\forall t$ . This design strategy endows the ARMA filters with a strong regularization that helps to prevent overfitting and greatly reduces the space complexity, in terms of trainable parameters.

To encourage each GCS stack to learn an  $\text{ARMA}_1$  filter with a response different from the ones learned by the other stacks, we apply stochastic dropout to the skip connections of the GCS layers. Finally, since the GCS stacks are independent, the computation of an ARMA layer can be distributed across multiple processing units.

### 3.1. Properties and relationship with other approaches

The ARMA layer can naturally deal with time-varying topologies and graph signals (Holme, 2015; Grattarola et al., 2019) by replacing the constant term  $\mathbf{X}$  in (11) with a time-dependent input  $\mathbf{X}^{(t)}$ .

Contrarily to filters defined in the spectral domain (Bruna et al., 2013), ARMA filters do not explicitly depend on the eigenvectors and the eigenvalues of  $\mathbf{L}$ , making them robust to perturbations in the underlying graph. For this reason, as formally proven for generic rational filters (Levie et al., 2019a), the proposed ARMA filters are stable and transferable, i.e., they can generalize to graph signals not seen during training and to graphs with different topologies.

Differently from polynomial filters, in the ARMA layer  $\mathbf{L}$  is not exponentiated and remains sparse. This implies much faster computations compared to Chebyshev filters (Defferrard et al., 2016), since  $\mathbf{L}^K$  becomes quickly dense. In particular,  $\mathbf{L}^K$  describes a fully connected graph if  $K$  is the graph diameter, which is usually small in real-world networks.



Unlike in a GCN (Kipf & Welling, 2016a), thanks to the skip connections it is possible to stack multiple GCS layers without risking to over-smooth the node features (Li et al., 2018). The weights sharing in the ARMA architecture shares similarities with a recurrent neural networks with residual connections (Wu et al., 2016). Similarly to GNNs operating directly in the node domain (Scarselli et al., 2009; Gallicchio & Micheli, 2010), each GCS layer computes the filtered signal  $\bar{\mathbf{x}}_i^{(t+1)}$  at vertex  $i$  as a combination of signals  $\mathbf{x}_j^{(t)}$  in its 1-hop neighborhood,  $j \in \mathcal{N}(i)$ . Such a commutative aggregation solves the problem of undefined vertex ordering and varying neighborhood sizes, making the proposed convolution operation permutation invariant. Finally, we note that the skip connections in ARMA inject in each GCS layer  $t$  of the stack the initial node features  $\mathbf{X}$ . This is different from a skip connection that either takes the output of the previous layer  $\mathbf{X}^{(t-1)}$  as input (Pham et al., 2017; Hamilton et al., 2017), or connects all the layers in a GNN stack directly to the output (Wu et al., 2018).

#### 4. Spectral analysis of the ARMA layer

The filter response of the ARMA filter derived in Sec. 2.2 cannot be exploited to analyze our GNN formulation, due to the presence of non-linearities. Therefore, we first recall that a filter changes the components of a graph signal  $\mathbf{X}$  on the eigenbase induced by  $\mathbf{L}$  (which is the same as in  $\bar{\mathbf{L}}$ , according to Sylvester’s theorem). Then, we investigate the effect of the proposed ARMA layer by taking the ratio of all the components of  $\mathbf{X}$  on the eigenbase before and after applying a stack of GCS layers. We define the *empirical filter response*  $\tilde{h}$  as

$$\tilde{h}_m = \frac{\mathbf{u}_m^T \bar{\mathbf{x}}_m}{\mathbf{u}_m^T \mathbf{x}_m}, \quad (13)$$

where  $\bar{\mathbf{x}}$  is a row of the GCS stack’s output  $\bar{\mathbf{X}}$  and  $\mathbf{u}$  is an eigenvector of  $\mathbf{L}$ . For visualization purposes, we train our GNN on a mono-dimensional graph signal  $\mathbf{X}$ , which is the 4<sup>th</sup> feature of the nodes in the Cora citation network (see the experiments for more details), and analyze the output of two GCS stacks in the ARMA layer. By using a single unit in the hidden layer, the matrices  $\mathbf{W}$  and  $\mathbf{V}$  in (11) reduce to the real values  $w$  and  $v$ . Hence, we can also compute  $h_{\text{ARMA}_1}$  analytically according to (9), by replacing  $a, b$  with  $w, v$ .

Fig. 2(a) depicts  $\tilde{h}$  after the 1<sup>st</sup>, 2<sup>nd</sup>, and 3<sup>rd</sup> layer in the first GCS stack and the filter response  $h_{\text{ARMA}_1}$  at convergence (black line). Clearly, with only 3 GCS layers is already possible to obtain a good approximation of the response of an ARMA<sub>1</sub> filter.

Fig. 2(d) shows how much the filter response  $\tilde{h}$ , resulting from a different number of GCS layers in the stack, modifies the Fourier components  $\mathbf{u}^T \bar{\mathbf{x}}$  of  $\bar{\mathbf{X}}$  associated to each

graph frequency. The quantities  $\tilde{h}$  and  $\mathbf{u}^T \bar{\mathbf{x}}$  obtained in a second GCS stack of our ARMA layer are depicted in Fig. 2(b,d). From these plots it emerges the powerful modeling capability of our ARMA layer that, by combining  $K$  different filter responses, can selectively shrink or amplify the Fourier components of the graph in many different ways.

We conclude our analysis by comparing the empirical response  $\tilde{h}$  resulting from a stack of GCNs, which is reported in Fig 2(c). As also highlighted by recent works (Wu et al., 2019; Maehara, 2019), the filtering obtained by stacking one or more GCNs has the undesired effect of symmetrically amplifying the lowest and also the highest frequencies of the spectrum. This is due to the GCN filter response, which is  $(1 - \lambda)^T$  in the linear case, and can assume negative values when  $T$  is odd. The effect is mitigated by summing  $\gamma \mathbf{I}_M$  to the adjacency matrix, which adds self-loops with weight  $\gamma$  and shrinks the spectral domain of the graph filter. For high values of  $\gamma$ , the GCN acts more as a low-pass filter that prevents high frequency oscillations. This is due to the presence of self loops, which limit the spread of information across the graph and the communication between neighbors.

However, even after adding  $\gamma \mathbf{I}_M$ , GCN cuts almost completely the medium frequencies and then amplifies again the higher ones, as shown in Fig. 2(f). Our ARMA filter, instead, can implement a filter response that gradually dampens the Fourier components as their frequency increases. Furthermore, as shown in Fig. 2(a,b), ARMA can learn different shapes of filter responses. On the other hand, the only degree of freedom to modify a GCN response consists in *manually* tuning the hyperparameter  $\gamma$ , to shrink the spectrum of the associated Laplacian.

#### 5. Experiments

We consider 4 downstream tasks: node classification, graph signal classification, graph classification, and graph regression. For a fair comparison, in all experiments we allow each filter to reach a node neighborhood of the same order on the graph. This is ensured by using the same polynomial order  $K$  for polynomial/rational filters, or by using a stack of  $K$  GCN layers. The details of every dataset considered in the experiments and the hyperparameters configuration for each model are deferred to the supplementary material.

##### 5.1. Semi-supervised node classification

First, we consider transductive node classification on 3 citation networks, Cora, Citeseer, and Pubmed. The input is a single graph described by an adjacency matrix  $\mathbf{A} \in \mathbb{R}^{M \times M}$ , the node features  $\mathbf{X} \in \mathbb{R}^{M \times F_{\text{in}}}$ , and the labels  $\mathbf{y}_l \in \mathbb{R}^{M_l}$  of a subset of nodes  $M_l \subset M$ . The targets

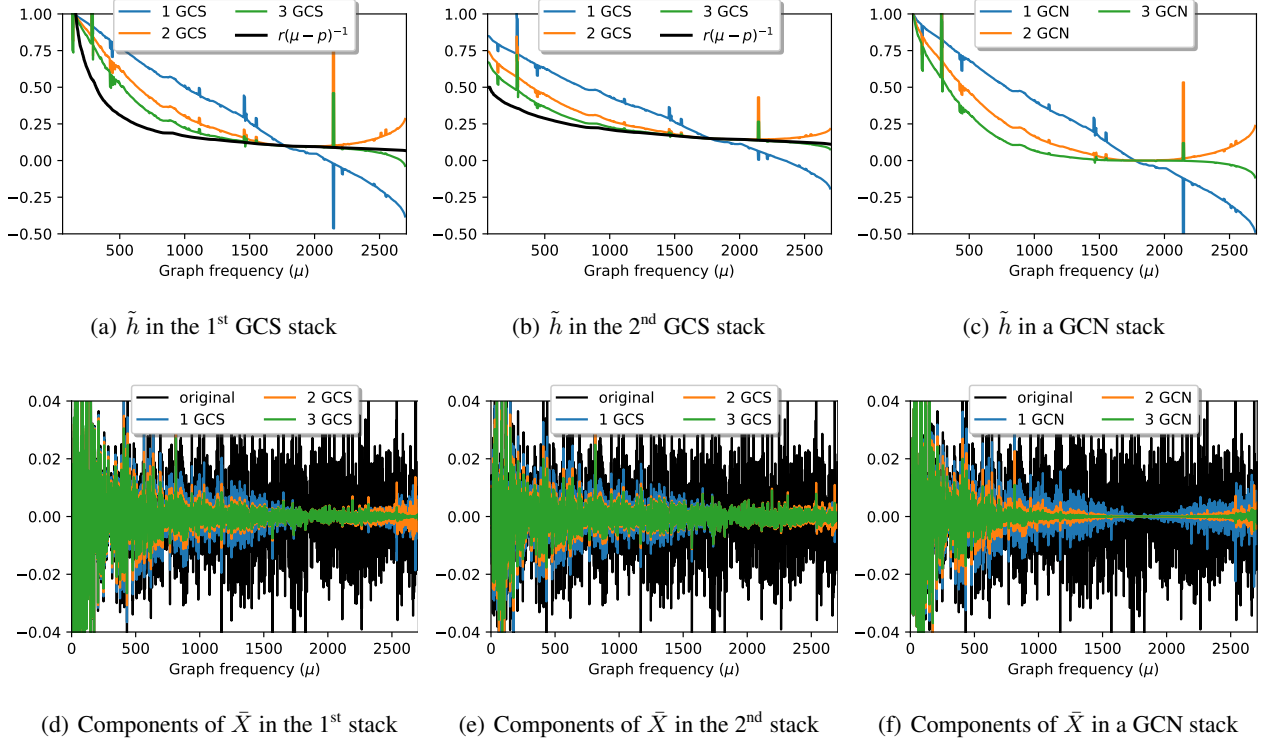


Figure 2. First row: empirical filter responses in two GCS stacks of an ARMA layer (a,b); black lines indicate the theoretical response at convergence. In (c), the empirical response of a stack of GCN layers. Second row: filtering effect of two GCS stacks in the ARMA filter (d,e) and of a stack of GCN layers (f) in the Fourier domain. Peaks are due to numerical imprecision in correspondence of tiny component values.

are the labels  $\mathbf{y}_u \in \mathbb{R}^{M_u}$  of the unlabelled nodes. The node features are sparse bag-of-words vectors representing text documents. The binary undirected edges in  $\mathbf{A}$  indicate citation links between documents. The models are trained using 20 labels per document class ( $\mathbf{y}_l$ ) and the performance is evaluated as classification accuracy on  $\mathbf{y}_u$ .

Secondly, we perform inductive node classification on the protein-protein interaction (PPI) network. The dataset consists of 20 graphs used for training, 2 for validation, and 2 for testing. Contrarily to the transductive setting, the testing graphs (and the associated node features) are unobserved during training. Additionally, each node can be associated to more than one class (multi-label classification).

We use a 2-layers GNN with 16 hidden units for the citation networks and 64 units for PPI. In the citation networks high dropout rates and  $L_2$ -norm regularization are exploited to prevent overfitting. Tab. 1 reports the classification accuracy obtained for GNN with different filters, namely a GNN equipped with the proposed ARMA filters, ChebNets (Defferrard et al., 2016), GCN (Kipf & Welling, 2016a), and CayleyNets (Levie et al., 2019b) that, like ARMA, implement rational spectral filters. As additional baselines,

we also include Graph Attention Networks (GAT) (Velickovic et al., 2017), GraphSAGE (Hamilton et al., 2017), and Graph Isomorphism Networks (GIN) (Xu et al., 2019).

Transductive node classification is a semi-supervised task that demands using a simple model with strong regularization to avoid overfitting on the few labels available. This is the key of GCN’s success when compared to more complex filters, such as ChebNet. Thanks to its flexible formulation, the proposed ARMA layer can implement the right degree of complexity and performs well on each task. On the other hand, since the PPI dataset is larger and more labels are available during training, less regularization is required and the models that are more complex are advantaged. This is reflected by the better performance achieved by ChebNets and CayleyNets, compared to GCNs. On PPI, ARMA significantly outperforms every other model, due to its powerful modelling capability that allows to learn filters with filter responses of different shapes.

Fig. 3 shows the training times of the GNN model configured with GCN, Chebyshev, Cayley, and ARMA layers. The Chebyshev filters computes powers of  $\mathbf{L}$  to reach higher-order neighborhoods, which translates in slow mul-

Figure 3. Training times on the PPI dataset. Times are recorded using an Nvidia GTX 2080.

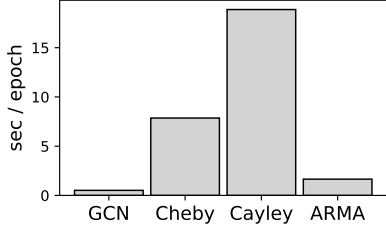


Table 1. Semi-supervised node classification accuracy.

Method	Cora	Citeseer	Pubmed	PPI
GAT	83.1 $\pm$ 0.6	70.9 $\pm$ 0.6	78.5 $\pm$ 0.3	81.3 $\pm$ 0.1
GrSage	73.7 $\pm$ 1.8	65.9 $\pm$ 0.9	78.5 $\pm$ 0.6	70.0 $\pm$ 0.0
GIN	75.1 $\pm$ 1.7	63.1 $\pm$ 2.0	77.1 $\pm$ 0.7	78.1 $\pm$ 2.6
GCN	81.5 $\pm$ 0.4	70.1 $\pm$ 0.7	<b>79.0 <math>\pm</math> 0.5</b>	80.8 $\pm$ 0.1
ChebNet	79.5 $\pm$ 1.2	70.1 $\pm$ 0.8	74.4 $\pm$ 1.1	86.4 $\pm$ 0.1
CayleyNet	81.2 $\pm$ 1.2	67.1 $\pm$ 2.4	75.6 $\pm$ 3.6	84.9 $\pm$ 1.2
<b>ARMA</b>	<b>83.4 <math>\pm</math> 0.6</b>	<b>72.5 <math>\pm</math> 0.4</b>	78.9 $\pm$ 0.3	<b>90.5 <math>\pm</math> 0.3</b>

tiplications with (almost) dense matrices. On the other hand, the ARMA layer exploits sparse operations that are linear in the number of nodes in  $\mathbf{L}$  and can be trained in a time comparable to the simple GCN architecture. Finally, CayleyNet is slower than the other methods, due to the complex formulation based on the Jacobi iterations.

## 5.2. Graph signal classification

In this task,  $N$  different graph signals  $\mathbf{X}_n \in \mathbb{R}^{M \times F_{in}}$ ,  $n = 1, \dots, N$ , defined on the same graph with adjacency matrix  $\mathbf{A} \in \mathbb{R}^{M \times M}$ , must be associated to labels  $y_1, \dots, y_N$ . We perform these experiments following the same setting of (Defferrard et al., 2016) for the MNIST and 20news datasets.

**MNIST.** To emulate a classic CNNs operating on a regular 2D grid, an 8-NN graph is defined on the 784 pixel of the MNIST images. The elements in  $\mathbf{A}$  are

$$a_{ij} = \exp\left(-\frac{\|p_i - p_j\|^2}{\sigma^2}\right), \quad (14)$$

where  $p_i$  and  $p_j$  are the 2D coordinates of pixel  $i$  and  $j$ . Each graph signal is a vectorized image  $\mathbf{x} \in \mathbb{R}^{784 \times 1}$ . The network architecture is GNN(32)-P(4)-GNN(64)-P(4)-FC(512)-FC<sub>Softmax</sub>(10), where GNN( $n$ ) indicates a GNN layer with  $n$  filters, P( $s$ ) a pooling operation with stride  $s$ , and FC( $u$ ) a fully connected layer with  $u$  units (the activation is specified as a subscript when relevant). Pooling is implemented by hierarchical clustering (GRACLUS) (Dhillon et al., 2004), which maps the graph signal  $\bar{\mathbf{x}}^{(l)}$  at layer  $l$  into a new node feature space  $\mathbf{x}^{(l+1)} \in$

Table 2. Graph signal classification accuracy.

GNN layer	MNIST	20news
GCN	98.48 $\pm$ 0.2	65.45 $\pm$ 0.2
ChebNet	99.14 $\pm$ 0.1	68.24 $\pm$ 0.2
CayleyNet	99.18 $\pm$ 0.1	68.84 $\pm$ 0.3
<b>ARMA</b>	<b>99.20 <math>\pm</math> 0.1</b>	<b>70.02 <math>\pm</math> 0.1</b>

$$\mathbb{R}^{M_{l+1} \times F_{l+1}}.$$

Tab. 2 reports the results obtained by using as filter ARMA, ChebNets, CayleyNets, or a stack of GCNs. The results are averaged over 10 runs and show that ARMA achieves a slightly higher (almost perfect) accuracy compared to Cheby and Cayley nets, while the performance of GCN is significantly lower.

**20news.** The dataset consists of 18,846 documents divided in 20 classes. Each graph signal is a document represented by a bag-of-words of the  $10^4$  most frequent words in the corpus, embedded via Word2vec (Mikolov et al., 2013). The underlying graph of  $10^4$  nodes is defined by a 16-NN adjacency matrix built as in Eq. (14), with the difference that  $p_i, p_j$  are now the embeddings of words  $i$  and  $j$ . We report results obtained with a single convolutional layer (GCN, ChebNet, CayleyNet, or ARMA), followed by global average pooling and softmax. As in (Defferrard et al., 2016), we use 32 filters for ChebNet. Instead, for GCN, CayleyNet and ARMA, better results are obtained with only 16 filters. The classification accuracy reported in Tab. 2 shows that ARMA significantly outperforms every other models also on this dataset.

## 5.3. Graph classification

In this task, the  $i$ -th datum is a graph represented by a pair  $\{\mathbf{A}_i, \mathbf{X}_i\}$ ,  $i = 1, \dots, N$ , where  $\mathbf{A}_i \in \mathbb{R}^{M_i \times M_i}$  is an adjacency matrix with  $M_i$  nodes, and  $\mathbf{X}_i \in \mathbb{R}^{M_i \times F}$  describes the node features. Each sample must be classified with a label  $y_i$ . We test the models on five different datasets. We use node degree, clustering coefficients, and node labels as additional node features. For each dataset we adopt a fixed network architecture GNN-GNN-GNN-AvgPool-FC<sub>Softmax</sub>, where AvgPool indicates a global average pooling layer. We compute the model performance over 10 runs, using 10% of the data for testing and 10% as validation data for early stopping. We report in Table 3 the average accuracy on the test set. For comparison, Tab. 3 also includes the results from GAT, GraphSAGE, and GIN. The GNN equipped with the proposed ARMA layer achieves the highest mean accuracy with respect to the polynomial filters (Cheby and GCN). Compared to CayleyNets, which are also based on a rational filter implementation, ARMA achieves not only a higher mean accuracy but also a lower

Table 3. Graph classification accuracy.

Method	Enzymes	Protein	D&D	MUTAG	BHard
GAT	51.7 $\pm$ 4.3	72.3 $\pm$ 3.1	70.9 $\pm$ 4.0	87.3 $\pm$ 5.3	30.1 $\pm$ 0.7
GrSage	60.3 $\pm$ 7.1	70.2 $\pm$ 3.9	73.6 $\pm$ 4.1	85.7 $\pm$ 4.7	71.8 $\pm$ 1.0
GIN	45.7 $\pm$ 7.7	71.4 $\pm$ 4.5	71.2 $\pm$ 5.4	86.3 $\pm$ 9.1	72.1 $\pm$ 1.1
GCN	53.0 $\pm$ 5.3	71.0 $\pm$ 2.7	74.7 $\pm$ 3.8	85.7 $\pm$ 6.6	71.9 $\pm$ 1.2
ChebNet	57.9 $\pm$ 2.6	72.1 $\pm$ 3.5	73.7 $\pm$ 3.7	82.6 $\pm$ 5.2	71.3 $\pm$ 1.2
CayleyNet	43.1 $\pm$ 10.7	65.6 $\pm$ 5.7	70.3 $\pm$ 11.6	87.8 $\pm$ 10.0	70.7 $\pm$ 2.4
<b>ARMA</b>	<b>60.6<math>\pm</math>7.2</b>	<b>73.7<math>\pm</math>3.4</b>	<b>77.6<math>\pm</math>2.7</b>	<b>91.5<math>\pm</math>4.2</b>	<b>74.1<math>\pm</math>0.5</b>

standard deviation. These empirical results indicate that our implementation is robust and, thus, confirm the hypothesis discussed in Sec. 3 about the stability and convergence of the proposed ARMA layer.

#### 5.4. Graph regression

This task is similar to graph classification, with the difference that the target output  $y_i$  is now a real value, rather than a discrete class label. We consider the QM9 chemical database (Ramakrishnan et al., 2014), which contains more than 130,000 molecular graphs. The nodes represent heavy atoms and the undirected edges the atomic bonds between them. Nodes have discrete attributes indicating one of four possible elements. The regression task consists in predicting a given chemical property of a molecule given its graph representation. As for graph classification, we evaluate the performance on randomly generated 80-10-10 train-validation-test splits. The network architecture adopted to predict each property is a GNN(64)-AvgPool-FC(128). We report in Tab. 4 the mean squared error (MSE) averaged over 10 independent runs, relative to the prediction of 9 molecular properties. It can be noticed that each model achieves a very low standard deviation. This is expected since the very large amount of training data allows the GNN to learn a configuration that generalizes well on the test set. Contrarily to the previous tasks, here there is not a clear winner among GCN, ChebNet, and CayleyNet, since each of them perform better than the other on some tasks. On the other hand, ARMA always achieves the lowest MSE in predicting each molecular property.

## 6. Conclusions

We proposed a novel graph convolutional layer based on a rational graph filter, which allows to model a more expressive filter response compared to polynomial filters. Our ARMA layer consists of parallel stacks of recurrent operations, which allow to approximate a graph filter with an arbitrary order  $K$ , by means of efficient sparse tensor multiplications. We reported a spectral analysis of our neural network implementation, which provides an insight on the

Table 4. Graph regression mean squared error.

Property	GCN	ChebNet	CayleyNet	ARMA
mu	0.445 $\pm$ 0.007	0.433 $\pm$ 0.003	0.442 $\pm$ 0.009	<b>0.394<math>\pm</math>0.005</b>
alpha	0.141 $\pm$ 0.016	0.171 $\pm$ 0.008	0.118 $\pm$ 0.005	<b>0.098<math>\pm</math>0.005</b>
HOMO	0.371 $\pm$ 0.030	0.391 $\pm$ 0.012	0.336 $\pm$ 0.007	<b>0.326<math>\pm</math>0.010</b>
LUMO	0.584 $\pm$ 0.051	0.528 $\pm$ 0.005	0.679 $\pm$ 0.148	<b>0.508<math>\pm</math>0.011</b>
gap	0.650 $\pm$ 0.070	0.565 $\pm$ 0.015	0.758 $\pm$ 0.106	<b>0.552<math>\pm</math>0.013</b>
R2	0.132 $\pm$ 0.005	0.294 $\pm$ 0.022	0.185 $\pm$ 0.043	<b>0.119<math>\pm</math>0.019</b>
ZPVE	0.349 $\pm$ 0.022	0.358 $\pm$ 0.001	0.555 $\pm$ 0.174	<b>0.338<math>\pm</math>0.001</b>
U0_atom	0.064 $\pm$ 0.003	0.126 $\pm$ 0.017	1.493 $\pm$ 1.414	<b>0.053<math>\pm</math>0.004</b>
Cv	0.192 $\pm$ 0.012	0.215 $\pm$ 0.010	0.184 $\pm$ 0.009	<b>0.163<math>\pm</math>0.007</b>

mechanisms behind the proposed layer and shows that our ARMA layer overcomes a known issue of simpler polynomial models like GCN. The experiments showed that the proposed ARMA layer is able to outperform existing GNN architectures, including those based on polynomial filters and other more complex models, on a large variety of graph machine learning tasks on graph data.

## References

- Bacciu, Davide, Errica, Federico, and Micheli, Alessio. Contextual graph markov model: A deep and generative approach to graph processing. In *Proceedings of the 35th international conference on Machine learning*. ACM, 2018.
- Battaglia, Peter W, Hamrick, Jessica B, Bapst, Victor, Sanchez-Gonzalez, Alvaro, Zambaldi, Vinicius, Malinowski, Mateusz, Tacchetti, Andrea, Raposo, David, Santoro, Adam, Faulkner, Ryan, et al. Relational inductive biases, deep learning, and graph networks. *arXiv preprint arXiv:1806.01261*, 2018.
- Bruna, Joan, Zaremba, Wojciech, Szlam, Arthur, and LeCun, Yann. Spectral networks and locally connected networks on graphs. *arXiv preprint arXiv:1312.6203*, 2013.
- Defferrard, Michaël, Bresson, Xavier, and Vandergheynst, Pierre. Convolutional neural networks on graphs with fast localized spectral filtering. In *Advances in Neural Information Processing Systems*, pp. 3844–3852, 2016.
- Dhillon, Inderjit S, Guan, Yuqiang, and Kulis, Brian. Kernel k-means: spectral clustering and normalized cuts. In *Proceedings of the tenth ACM SIGKDD international conference on Knowledge discovery and data mining*, pp. 551–556. ACM, 2004.
- Duvenaud, David K, Maclaurin, Dougal, Iparraguirre, Jorge, Bombarell, Rafael, Hirzel, Timothy, Aspuru-Guzik, Alán, and Adams, Ryan P. Convolutional networks on graphs for learning molecular fingerprints. In



- Advances in neural information processing systems*, pp. 2224–2232, 2015.
- Gallicchio, Claudio and Micheli, Alessio. Graph echo state networks. In *Neural Networks (IJCNN), The 2010 International Joint Conference on*, pp. 1–8. IEEE, 2010.
- Grattarola, Daniele, Zambon, Daniele, Alippi, Cesare, and Livi, Lorenzo. Change detection in graph streams by learning graph embeddings on constant-curvature manifolds. *IEEE Transactions on neural networks and learning systems*, 2019.
- Hamilton, Will, Ying, Zhitao, and Leskovec, Jure. Inductive representation learning on large graphs. In *Advances in Neural Information Processing Systems*, pp. 1024–1034, 2017.
- Henaff, Mikael, Bruna, Joan, and LeCun, Yann. Deep convolutional networks on graph-structured data. *arXiv preprint arXiv:1506.05163*, 2015.
- Holme, Petter. Modern temporal network theory: a colloquium. *The European Physical Journal B*, 88(9):234, 2015.
- Isufi, Elvin, Loukas, Andreas, Simonetto, Andrea, and Leus, Geert. Autoregressive moving average graph filtering. *arXiv preprint arXiv:1602.04436*, 2016.
- Kipf, Thomas N and Welling, Max. Semi-supervised classification with graph convolutional networks. In *International Conference on Learning Representations (ICLR)*, 2016a.
- Kipf, Thomas N and Welling, Max. Variational graph auto-encoders. In *NIPS Workshop on Bayesian Deep Learning*, 2016b.
- Klicpera, Johannes, Bojchevski, Aleksandar, and Günnemann, Stephan. Predict then propagate: Graph neural networks meet personalized pagerank. In *International Conference on Learning Representations (ICLR)*, 2019.
- Levie, Ron, Elvin, Isufi, and Gitta, Kutyniok. On the transferability of spectral graph filters. *arXiv preprint*, 2019a.
- Levie, Ron, Monti, Federico, Bresson, Xavier, and Bronstein, Michael M. Cayleynets: Graph convolutional neural networks with complex rational spectral filters. *IEEE Transactions on Signal Processing*, 67(1):97–109, Jan 2019b. ISSN 1053-587X. doi: 10.1109/TSP.2018.2879624.
- Li, Qimai, Han, Zhichao, and Wu, Xiao-Ming. Deeper insights into graph convolutional networks for semi-supervised learning. In *Proceedings of AAAI Conference on Artificial Intelligence*, 2018.
- Liao, Renjie, Zhao, Zhizhen, Urtasun, Raquel, and Zemel, Richard. Lanczosnet: Multi-scale deep graph convolutional networks. In *International Conference on Learning Representations (ICLR)*, 2019.
- Loukas, Andreas, Simonetto, Andrea, and Leus, Geert. Distributed autoregressive moving average graph filters. *IEEE Signal Processing Letters*, 22(11):1931–1935, 2015.
- Maehara, Takanori. Revisiting graph neural networks: All we have is low-pass filters. *arXiv preprint arXiv:1905.09550*, 2019.
- Mikolov, Tomas, Chen, Kai, Corrado, Greg, and Dean, Jeffrey. Efficient estimation of word representations in vector space. In *ICLR (Workshop)*, 2013.
- Narang, Sunil K, Gadde, Akshay, and Ortega, Antonio. Signal processing techniques for interpolation in graph structured data. In *Acoustics, Speech and Signal Processing (ICASSP), 2013 IEEE International Conference on*, pp. 5445–5449. IEEE, 2013.
- Page, Lawrence, Brin, Sergey, Motwani, Rajeev, and Winograd, Terry. The pagerank citation ranking: Bringing order to the web. Technical report, Stanford InfoLab, 1999.
- Perozzi, Bryan, Al-Rfou, Rami, and Skiena, Steven. Deepwalk: Online learning of social representations. In *Proceedings of the 20th ACM SIGKDD international conference on Knowledge discovery and data mining*, pp. 701–710. ACM, 2014.
- Pham, Trang, Tran, Truyen, Phung, Dinh, and Venkatesh, Svetha. Column networks for collective classification. In *Thirty-First AAAI Conference on Artificial Intelligence*, 2017.
- Ramakrishnan, Raghunathan, Dral, Pavlo O, Rupp, Matthias, and Von Lilienfeld, O Anatole. Quantum chemistry structures and properties of 134 kilo molecules. *Scientific data*, 1:140022, 2014.
- Scarselli, Franco, Gori, Marco, Tsoi, Ah Chung, Hagenbuchner, Markus, and Monfardini, Gabriele. The graph neural network model. *IEEE Transactions on Neural Networks*, 20(1):61–80, 2009.
- Shuman, David I, Vandergheynst, Pierre, and Frossard, Pascal. Chebyshev polynomial approximation for distributed signal processing. In *Distributed Computing in Sensor Systems and Workshops (DCOSS), 2011 International Conference on*, pp. 1–8. IEEE, 2011.
- Susnjara, Ana, Perraudin, Nathanael, Kressner, Daniel, and Vandergheynst, Pierre. Accelerated filtering on graphs using lanczos method. *arXiv preprint arXiv:1509.04537*, 2015.

- Tremblay, Nicolas, Goncalves, Paulo, and Borgnat, Pierre. Design of graph filters and filterbanks. In *Cooperative and Graph Signal Processing*, pp. 299–324. Elsevier, 2018.
- Velickovic, Petar, Cucurull, Guillem, Casanova, Aran-txa, Romero, Adriana, Lio, Pietro, and Bengio, Yoshua. Graph attention networks. *arXiv preprint arXiv:1710.10903*, 2017.
- Wu, Felix, Zhang, Tianyi, Souza Jr, Amauri Holanda de, Fifty, Christopher, Yu, Tao, and Weinberger, Kilian Q. Representation learning on graphs with jumping knowledge networks. In *Proceedings of the 35th International Conference on International Conference on Machine Learning*. JMLR. org, 2018.
- Wu, Felix, Zhang, Tianyi, Souza Jr, Amauri Holanda de, Fifty, Christopher, Yu, Tao, and Weinberger, Kilian Q. Simplifying graph convolutional networks. In *Proceedings of the 36th International Conference on International Conference on Machine Learning*. JMLR. org, 2019.
- Wu, Yonghui, Schuster, Mike, Chen, Zhifeng, Le, Quoc V, Norouzi, Mohammad, Macherey, Wolfgang, Krikun, Maxim, Cao, Yuan, Gao, Qin, Macherey, Klaus, et al. Google’s neural machine translation system: Bridging the gap between human and machine translation. *arXiv preprint arXiv:1609.08144*, 2016.
- Xu, Keyulu, Hu, Weihua, Leskovec, Jure, and Jegelka, Stefanie. How powerful are graph neural networks? In *International Conference on Learning Representations (ICLR)*, 2019.
- Yang, Zhilin, Cohen, William W, and Salakhutdinov, Ruslan. Revisiting semi-supervised learning with graph embeddings. In *Proceedings of the 33rd International Conference on International Conference on Machine Learning-Volume 48*, pp. 40–48. JMLR. org, 2016.
- Zhang, Muhan, Cui, Zhicheng, Neumann, Marion, and Chen, Yixin. An end-to-end deep learning architecture for graph classification. In *Proceedings of AAAI Conference on Artificial Intelligence*, 2018.
- Zhou, Denny, Bousquet, Olivier, Lal, Thomas N, Weston, Jason, and Schölkopf, Bernhard. Learning with local and global consistency. In *Advances in neural information processing systems*, pp. 321–328, 2004.

## Supplementary material

### Node classification

The statistics of the node classification datasets are reported in Tab. 5. The three citation networks (Cora, Citeseer, and Pubmed) are taken from <https://github.com/tkipf/gcn/raw/master/gcn/data/>, while the PPI dataset is taken from <http://snap.stanford.edu/graphsage/>.

Table 5. Details of the node classification datasets

Dataset	Nodes	Edges	Node attr.	Node classes
Cora	2708	5429	1433	7 (single label)
Citeseer	3327	9228	3703	6 (single label)
Pubmed	19717	88651	500	3 (single label)
PPI	56944	818716	50	121 (multi-label)

Table 6. Hyperparameters used in node classification.

Dataset	$L_2$ reg.	$p_{\text{drop}}$	lr	GCN $L$	ChebNet $K$	CayleyNet $K$ # Jacob. it.	ARMA $[K, T]$
Cora	5e-4	0.75	1e-2	1	2	1 5	[2,1]
Citeseer	5e-4	0.75	1e-2	1	3	1 5	[3,1]
Pubmed	5e-4	0.25	1e-2	1	3	2 5	[1,1]
PPI	0.0	0.25	1e-2	2	3	3 5	[3,2]

Tab. 6 describes the optimal hyperparameters used in GCN, ChebNet, CayleyNet and ARMA for each node classification dataset. For all GNN, we report the  $L_2$  regularization weight, the learning rate (lr) and dropout probability ( $p_{\text{drop}}$ ). For GCN, we report the number of stacked graph convolutions ( $L$ ). For ChebNet, we report the polynomial order ( $K$ ). For CayleyNet, we report the polynomial order ( $K$ ) and the number of Jacobi iterations. For ARMA, we report number of GCS stacks ( $K$ ), and stack’s depth ( $T$ ). Additionally, we configured the MLP in GIN with 2 hidden layers and trained the parameter  $\epsilon$ , while for GRAPHSAGE we used the *max* aggregator, to differentiate more its behavior from GCN and GIN. Finally, GAT is configured with 8 attention heads and the same number of layers  $L$  as GCN.

Each model is trained for 2000 epochs with early stopping (based on the validation accuracy) at 50 epochs. We used full-batch training, i.e., in each epoch the weights are updated one time, according to a single batch that includes all the training data.

### Graph signal classification

To generate the datasets we used the code available at [github.com/mdeff/cnn\\_graph](https://github.com/mdeff/cnn_graph). The models are trained for 20 epochs on each dataset. We used batches of size 32 for MNIST and 128 for 20news. In the 20news dataset, the words are embedded in vectors of size 200.

Table 7. Details of the graph signal classification datasets.

Dataset	Nodes	Edges	Classes	Tr. samples	Val. samples	Test samples
MNIST	784	5,928	10	55,000	5,000	10,000
20news	10,000	249,944	20	10,168	7,071	7,071

Table 8. Hyperparameters used in graph signal classification.

Dataset	$L_2$ reg.	lr	$p_{\text{drop}}$	GCN $L$	ChebNet $K$	CayleyNet $K$ # Jacob. it.	ARMA $[K, T]$
MNIST	5e-4	1e-3	0.5	3	25	12 11	[5,10]
20news	1e-3	1e-3	0.7	1	5	5 10	[1,1]

The statistics of the graph signal classification datasets are reported in Tab. 7, while Tab. 8 reports the optimal hyperparameters configuration for each model.

### Graph classification

The datasets Enzymes, Proteins, D&D, and MUTAG are taken from the repository Benchmark Data Sets for Graph Kernels <https://ls11-www.cs.tu-dortmund.de/staff/morris/graphkerneldatasets>, while the dataset Bench-hard is taken from [https://github.com/FilippoMB/Benchmark\\_dataset\\_for\\_graph\\_classification](https://github.com/FilippoMB/Benchmark_dataset_for_graph_classification). The statistics of each graph classification dataset are summarized in Tab. 9.

For all methods, we use a fixed architecture composed of three GNN layers, each with 32 output units, ReLU activations, and  $L_2$  regularization with a factor of  $10^{-4}$ . All models are trained to convergence with Adam, using a learning rate of  $10^{-3}$ , batch size of 32, and a patience of 50 epochs. We summarize in Table 10 the hyperparameters used for ARMA, ChebNets, and CayleyNets on the different datasets.

Table 9. Summary of statistics of the graph classification datasets

Dataset	Samples	Classes	Avg. nodes	Avg. edges	Node attr.	Node labels
Bench-hard	1,800	3	148.32	572.32	–	yes
Enzymes	600	6	32.63	62.14	18	no
Proteins	1,113	2	39.06	72.82	1	no
D&D	1,178	2	284.32	715.66	–	yes
MUTAG	188	2	17.93	19.79	–	yes

Table 10. Hyperparameters for graph classification and graph regression.

Dataset	GCN	ChebNet	CayleyNet		ARMA		
	$L$	$K$	$K$	Jacobi iters.	$p_{drop}$	$K$	$T$
Bench-hard	2	2	2	10	0.4	1	2
Enzymes	2	2	2	10	0.6	2	2
Proteins	4	4	4	10	0.6	4	4
D&D	4	4	4	10	0.0	4	4
MUTAG	4	4	4	10	0.0	4	4

### Graph regression

The QM9 dataset used for graph regression is available at <http://quantum-machine.org/datasets/>, and its statistics are reported in Tab. 11.

The hyperparameters are reported in Tab. 12. Only for this task, CayleyNets use only 3 Jacobi iterations, since with more iterations we experienced numerical errors and the loss quickly diverged. All models are trained for 1000 epochs with early stopping at 50 epochs, using Adam optimizer with initial learning rate  $1e-3$ . We used batch size 64 and no  $L_2$  regularization.

Table 11. Summary of statistics of the graph regression dataset

Samples	Avg. nodes	Avg. edges	Node attr.
133,885	8.79	27.61	1 ( $\in \mathbb{N}^4$ )

Table 12. Hyperparameters for graph classification and graph regression.

Dataset	GCN	ChebNet	CayleyNet		ARMA		
	$L$	$K$	$K$	Jacobi iters.	$p_{drop}$	$K$	$T$
QM9	3	3	3	3	0.75	3	3